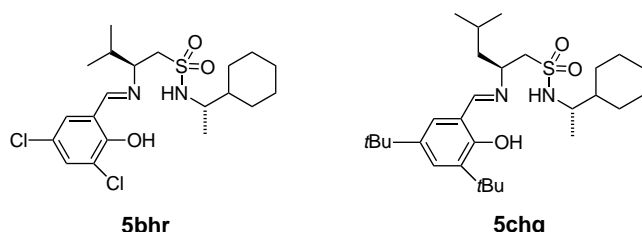


Table 1. High-throughput screening of the library of ligands **5**: best ten results.

Entry	Ligand	R <sup>1</sup>	R <sup>2</sup>	R <sup>3</sup>	ee ( <b>12</b> ) [%]	ee ( <b>13</b> ) [%]
1	<b>5bhr</b>	<i>i</i> Pr	( <i>S</i> )-CH(Me)Cy	3,5-Cl <sub>2</sub>	82	81
2	<b>5ehq</b>	<i>t</i> Bu	( <i>S</i> )-CH(Me)Cy	3,5- <i>t</i> Bu <sub>2</sub>	80	79
3	<b>5biq</b>	<i>i</i> Pr	<i>i</i> Pr	3,5- <i>t</i> Bu <sub>2</sub>	76	72
4	<b>5ejq</b>	<i>t</i> Bu	CHPh <sub>2</sub>	3,5- <i>t</i> Bu <sub>2</sub>	74	75
5	<b>5chr</b>	<i>i</i> Bu	( <i>S</i> )-CH(Me)Cy	3,5-Cl <sub>2</sub>	73	74
6	<b>5chq</b>	<i>i</i> Bu	( <i>S</i> )-CH(Me)Cy	3,5- <i>t</i> Bu <sub>2</sub>	72	71
7	<b>5aiq</b>	Me	<i>i</i> Pr	3,5- <i>t</i> Bu <sub>2</sub>	69	76
8	<b>5ehs</b>	<i>t</i> Bu	( <i>S</i> )-CH(Me)Cy	(CH) <sub>4</sub>	71	71
9	<b>5bjq</b>	<i>i</i> Pr	CHPh <sub>2</sub>	3,5- <i>t</i> Bu <sub>2</sub>	70	69
10	<b>5chr</b>	<i>t</i> Bu	( <i>S</i> )-CH(Me)Cy	3,5-Cl <sub>2</sub>	71	67

Under the best conditions (2.75 mol % **5**, 2.5 mol % Cu(OTf)<sub>2</sub>, toluene/hexane 80/20, 5 h), **5bhr** was identified as the best ligand for cyclohexenone **9** and cycloheptenone **10**



(at –20 °C), giving **12** in 90 % ee and **13** in 85 % ee, with 100 % conversion in both cases and 93–95 % yield (isolated product). Compound **5chq** (Figure 1) was recognized as the best ligand for cyclopentenone (**11**) (at 0 °C), giving **14** in 80 % ee albeit in a low yield (25 %).

In conclusion, we have developed a parallel library of new Schiff base chiral ligands **5** and optimized their use in the enantioselective conjugate addition of Et<sub>2</sub>Zn to cyclic enones by a high-throughput screening approach. Work is in progress to extend the scope of ligands **5** in other enantioselective reactions.

Received: October 14, 1999 [Z14150]

- [1] a) P. Perlmutter in *Conjugate Addition Reactions in Organic Synthesis*, Vol. 9 (Eds.: J. E. Baldwin, P. D. Magnus), Tetrahedron Organic Chemistry Series, Pergamon, Oxford, **1992**; b) Y. Yamamoto, *Methoden Org. Chem. (Houben-Weyl)* 4th ed. 1995–, Vol. E21b, Vol. 4, **1995**, chap. 1.5.2.1.
- [2] a) B. E. Rossiter, N. M. Swingle, *Chem. Rev.* **1992**, 92, 771–806; b) N. Krause, A. Gerold, *Angew. Chem.* **1997**, 109, 194–213; *Angew. Chem. Int. Ed. Engl.* **1997**, 36, 186–204; c) B. L. Feringa, A. H. M. de Vries in *Advances in Catalytic Processes*, Vol. 1 (Ed.: M. P. Doyle), JAI, Greenwich, CT, **1995**, pp. 151–192.
- [3] a) Although the mechanistic path for this reaction has not yet been completely clarified, it is likely that mixed (Cu–Zn) organometallic species are involved in the catalytic step. For a brief review, see: N. Krause, *Angew. Chem.* **1998**, 110, 295–297; *Angew. Chem. Int. Ed.* **1998**, 37, 283–285; b) R. Naasz, L. A. Arnold, M. Pineschi, E. Keller, B. L. Feringa, *J. Am. Chem. Soc.* **1999**, 121, 1104–1105, and references therein; c) A. K. H. Knöbel, I. H. Escher, A. Pfalz, *Synlett* **1997**, 1429; d) A. Alexakis, J. Vastra, J. Burton, C. Benhaim, P. Mangeney, *Tetrahedron Lett.* **1998**, 39, 7869–7872, and references therein; e) O. Pamies, G. Net, A. Ruiz, C. Claver, *Tetrahedron: Asymmetry* **1999**, 10, 2007–2014; f) M. Yan, A. S. C. Chan, *Tetrahedron Lett.* **1999**, 40, 6645–6648; g) T. Mori, K. Kosaka, Y. Nakagawa, Y. Nagaoka, K. Tomioka, *Tetrahedron: Asymmetry* **1998**, 9, 3175–3178.

- [4] a) M. Kitamura, T. Miki, K. Nakano, R. Noyori, *Tetrahedron Lett.* **1996**, 37, 5141–5144; b) V. Wendisch, N. Sewald, *Tetrahedron: Asymmetry* **1997**, 8, 1253–1257.
- [5] a) M. Gude, U. Piarulli, D. Potenza, B. Salom, C. Gennari, *Tetrahedron Lett.* **1996**, 37, 8589–8592; b) C. Gennari, M. Gude, D. Potenza, U. Piarulli, *Chem. Eur. J.* **1998**, 4, 1924–1931.
- [6] The absolute configuration shown in Scheme 2 for **12** (3*S*) was determined by <sup>13</sup>C NMR spectroscopy after derivatization with (1*R*,2*R*) 1,2-diphenylethylenediamine (A. Alexakis, J. C. Frutos, P. Mangeney, *Tetrahedron: Asymmetry* **1993**, 4, 2431–2434). The absolute configuration of **13** is unknown. The absolute configuration of **14** (3*S*) was determined by optical rotation: G. H. Posner, M. Hulce, *Tetrahedron Lett.* **1984**, 25, 379–382.
- [7] For reviews on the combinatorial development of new catalysts, see: a) C. Gennari, H. P. Nestler, U. Piarulli, B. Salom, *Liebigs Ann.* **1997**, 637–647; b) K. D. Shimizu, M. L. Snapper, A. H. Hoveyda, *Chem. Eur. J.* **1998**, 4, 1885–1889; c) B. Jandeleit, D. J. Schaefer, T. S. Powers, H. W. Turner, W. H. Weinberg, *Angew. Chem.* **1999**, 111, 2648–2689; *Angew. Chem. Int. Ed.* **1999**, 38, 2494–2532, and references therein.
- [8] C. Gennari, S. Ceccarelli, U. Piarulli, C. A. G. N. Montalbetti, R. F. W. Jackson, *J. Org. Chem.* **1998**, 63, 5312–5313.
- [9] a) R. M. Lawrence, S. A. Biller, O. M. Fryszman, M. A. Poss, *Synthesis* **1997**, 553–558; b) D. L. Flynn, J. Z. Crich, R. V. Devraj, S. L. Hockerman, J. J. Parlow, M. S. South, S. Woodard, *J. Am. Chem. Soc.* **1997**, 119, 4874–4881; c) R. J. Booth, J. C. Hodges, *J. Am. Chem. Soc.* **1997**, 119, 4882–4886; d) J. J. Parlow, D. A. Mischke, S. S. Woodard, *J. Org. Chem.* **1997**, 62, 5908–5919; e) J. J. Parlow, D. L. Flynn, *Tetrahedron* **1998**, 54, 4013–4031.
- [10] Polymer-bound “dimethylaminopyridine” (4-(*N*-benzyl-*N*-methylamino)pyridine on polystyrene) is commercially available from the Aldrich Chemical Company.
- [11] X. Gao, H. B. Kagan, *Chirality* **1998**, 10, 120–124.
- [12] B. M. Cole, K. D. Shimizu, C. A. Krueger, J. P. A. Harrity, M. L. Snapper, A. H. Hoveyda, *Angew. Chem.* **1996**, 108, 1776–1779; *Angew. Chem. Int. Ed. Engl.* **1996**, 35, 1668–1671.

## The Melting Point Alternation in $\alpha,\omega$ -Alkanediols and $\alpha,\omega$ -Alkanediamines: Interplay between Hydrogen Bonding and Hydrophobic Interactions\*\*

Venkat R. Thalladi, Roland Boese,\* and Hans-Christoph Weiss

Dedicated to Professor Paul Rademacher on the occasion of his 60th birthday

Hydrogen bonding and hydrophobic interactions are ubiquitous in biological structures, be they lipids, proteins, or nucleic acids.<sup>[1]</sup> The interference between these two kinds of interactions in such natural systems is obvious, but hard to study and difficult to perceive owing to their inherent complexity. An understanding of such interference has important implications in biological and material phenom-

[\*] Prof. Dr. R. Boese, Dr. V. R. Thalladi, Dipl.-Chem. H.-C. Weiss  
Institut für Anorganische Chemie  
Universität-GH Essen  
Universitätsstrasse 5–7, 45117 Essen (Germany)  
Fax: (+49)201-183-2535  
E-mail: boese@structchem.uni-essen.de

[\*\*] The Melting Point Alternation in *n*-Alkanes and Derivatives, Part 2. This work was supported by the Deutsche Forschungsgemeinschaft and the Fonds der Chemischen Industrie. V.R.T. thanks the Alexander von Humboldt Foundation for a postdoctoral fellowship. Part 1: ref. [6].

ena.<sup>[2]</sup> Described here are the structural details of  $\alpha,\omega$ -alkanediols and  $\alpha,\omega$ -alkanediamines (named diols and diamines hereafter) which are characterized by hydrogen bonding and hydrophobic interactions. These systems represent a balance between structural simplicity and interaction complexity, which makes the study of interference between interactions a feasible exercise.<sup>[3]</sup>

The melting point alternation in  $n$ -alkanes and most end-substituted  $n$ -alkanes has been known for decades.<sup>[4, 5]</sup> Physical properties such as solubilities and sublimation enthalpies that are related to the solid state also exhibit an alternating pattern, whereas those related to the liquid state show monotonic behavior.<sup>[5]</sup>  $n$ -Alkanes are solely held together by hydrophobic interactions in the solid state, and we have shown recently that the melting point alternation in  $n$ -alkanes can be explained in terms of a simple geometrical model.<sup>[6]</sup> We have now undertaken a structural study of the diols  $\text{HO}-(\text{CH}_2)_n-\text{OH}$  ( $n=2-10$ ) and the diamines  $\text{H}_2\text{N}-(\text{CH}_2)_n-\text{NH}_2$  ( $n=2-8$ ). Most of these are liquids at room temperature, and their single crystals have been grown in situ using a miniature zone melting procedure with an IR laser.<sup>[7]</sup> The melting points were recorded by differential scanning calorimetry and no indications of phase transitions were found. The melting point alternation is shown in Figure 1a. The X-ray data (Table 1) for all the compounds were collected at the same temperature (130 K) to allow a comparison of calculated densities.<sup>[8, 9]</sup> The density gives a measure of compactness in packing and in a homologous series it may be correlated with the melting point.<sup>[6]</sup> Figure 1b shows that the odd-numbered members (named odd hereafter) are more poorly packed than the even-numbered members (named even hereafter) in both series. The even diols with  $n \geq 4$  form a layerlike network (space groups  $P2_1/n$  and  $P2_1/c$ ), and the odd members form a three-dimensional structure (space group  $P2_12_12_1$ ). This result is against the intuition that a three-dimensional network should have a higher melting point than a two-dimensional network.

The end groups in the diols and diamines form hydrogen bonds, and the alkyl chains participate in hydrophobic interactions. Therefore our analysis seeks to find the relevant

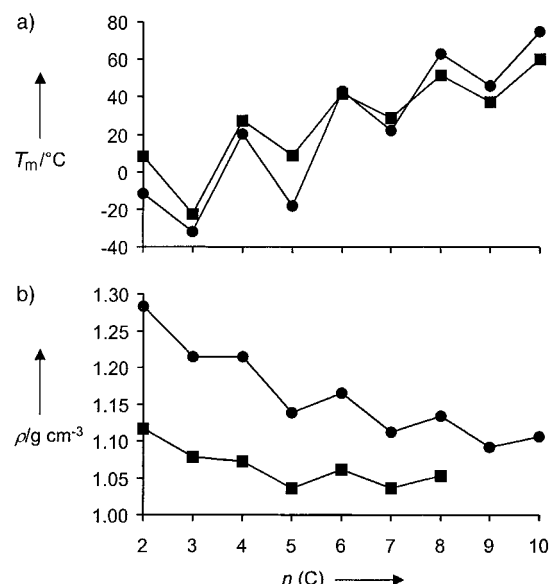


Figure 1. Alternation in the melting point  $T_m$  (a) and density  $\rho$  (b) in diols (●) and diamines (■) with increasing number of C atoms  $n(C)$ .

requirements for hydrogen bonding and hydrophobic interactions and establish their mutual dependence. The common packing pattern in both even and odd  $n$ -alkanes is a columnar structure wherein the molecules are stacked such that  $\text{CH}_2$  groups of successive molecules are intergrooved (Figure 2).<sup>[6]</sup> Typically, such a close packing of the  $\text{CH}_2$  groups occurs at an intermolecular separation of 4.7 Å.

Since OH groups act as hydrogen-bond donors and acceptors simultaneously, they form several types of supramolecular synthons,<sup>[3]</sup> the most common of which is a chain pattern.<sup>[10]</sup> If  $\text{O}-\text{H} \cdots \text{O}$  chains are formed at both ends of the molecule, a layer structure consisting of molecules in columns can be anticipated (Figure 3a).<sup>[11]</sup> Given the  $\text{O}-\text{H} \cdots \text{O}$  geometry, successive molecules in a column are then separated by 5.1 Å, a distance that is too long for the hydrophobic packing observed in  $n$ -alkanes. However, the layer structure of the even diols circumvents this problem in an exquisite fashion

Table 1. Important structural information of diols and diamines.

Compound	Space group	Z	Lattice parameters			$C_k^*$	Lattice energy [kcal mol <sup>-1</sup> ]		
			<i>a</i> [Å]	<i>b</i> [Å]	<i>c</i> [Å]		$\beta$ [°]	H-bond	van der Waals
HO(CH <sub>2</sub> ) <sub>2</sub> OH	<i>P</i> 2 <sub>1</sub> 2 <sub>1</sub> 2 <sub>1</sub>	4	5.0130	6.9149	9.2710	90	0.693	− 7.675	− 5.735
HO(CH <sub>2</sub> ) <sub>3</sub> OH	<i>P</i> 2 <sub>1</sub> / <i>n</i>	4	4.9396	7.9436	10.6007	90.097	0.698	− 7.623	− 7.282
HO(CH <sub>2</sub> ) <sub>4</sub> OH	<i>P</i> 2 <sub>1</sub> / <i>n</i>	4	5.0135	13.7880	7.4635	107.275	0.708	− 7.713	− 10.935
HO(CH <sub>2</sub> ) <sub>5</sub> OH	<i>P</i> 2 <sub>1</sub> 2 <sub>1</sub> 2 <sub>1</sub>	4	5.3234	6.6991	17.0398	90	0.672	− 7.772	− 11.014
HO(CH <sub>2</sub> ) <sub>6</sub> OH	<i>P</i> 2 <sub>1</sub> / <i>n</i>	4	7.8676	5.0554	16.9653	93.454	0.714	− 7.536	− 15.018
HO(CH <sub>2</sub> ) <sub>7</sub> OH	<i>P</i> 2 <sub>1</sub> 2 <sub>1</sub> 2 <sub>1</sub>	4	5.1698	6.8442	22.3214	90	0.680	− 7.528	− 15.889
HO(CH <sub>2</sub> ) <sub>8</sub> OH	<i>P</i> 2 <sub>1</sub> / <i>n</i>	2	4.7995	5.0846	17.5408	90.315	0.710	− 7.726	− 19.813
HO(CH <sub>2</sub> ) <sub>9</sub> OH	<i>P</i> 2 <sub>1</sub> 2 <sub>1</sub> 2 <sub>1</sub>	4	5.1118	6.9409	27.4620	90	0.682	− 7.577	− 21.028
HO(CH <sub>2</sub> ) <sub>10</sub> OH <sup>[a]</sup>	<i>P</i> 2 <sub>1</sub> / <i>c</i>	2	4.799	5.113	21.029	93.37	0.714	− 7.028	− 23.898
H <sub>2</sub> N(CH <sub>2</sub> ) <sub>2</sub> NH <sub>2</sub>	<i>P</i> 2 <sub>1</sub> / <i>c</i>	2	5.0467	7.1552	5.4746	115.363	0.717	− 3.579	− 8.421
H <sub>2</sub> N(CH <sub>2</sub> ) <sub>3</sub> NH <sub>2</sub>	<i>Cmc</i> 2 <sub>1</sub>	4	12.6191	6.1297	5.9074	90	0.694	− 4.982	− 9.413
H <sub>2</sub> N(CH <sub>2</sub> ) <sub>4</sub> NH <sub>2</sub>	<i>Pbca</i>	4	6.5516	5.7382	14.5275	90	0.698	− 5.224	− 12.358
H <sub>2</sub> N(CH <sub>2</sub> ) <sub>5</sub> NH <sub>2</sub>	<i>Cmc</i> 2 <sub>1</sub>	4	17.7088	6.2282	5.8572	90	0.688	− 4.972	− 13.657
H <sub>2</sub> N(CH <sub>2</sub> ) <sub>6</sub> NH <sub>2</sub>	<i>Pbca</i>	4	6.7607	5.6643	19.0030	90	0.698	− 4.923	− 17.316
H <sub>2</sub> N(CH <sub>2</sub> ) <sub>7</sub> NH <sub>2</sub>	<i>Cmc</i> 2 <sub>1</sub>	4	22.8133	6.3654	5.7511	90	0.677	− 4.938	− 18.223
H <sub>2</sub> N(CH <sub>2</sub> ) <sub>8</sub> NH <sub>2</sub>	<i>Pbca</i>	4	6.8928	5.6101	23.5274	90	0.692	− 4.932	− 22.387

[a] The packing fraction ( $C_k^*$ ) and lattice energies given for this compound<sup>[2a]</sup> are extrapolated to 130 K.

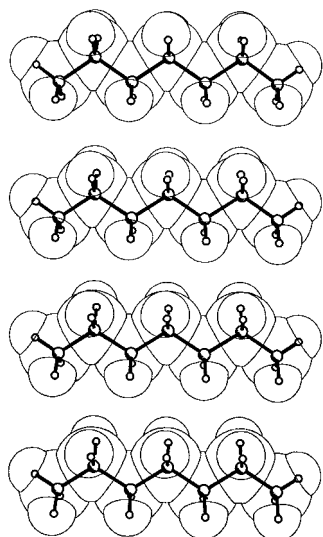


Figure 2. Columnar structure in *n*-heptane revealing the typical intergrooving pattern of  $\text{CH}_2$  groups in *n*-alkanes.

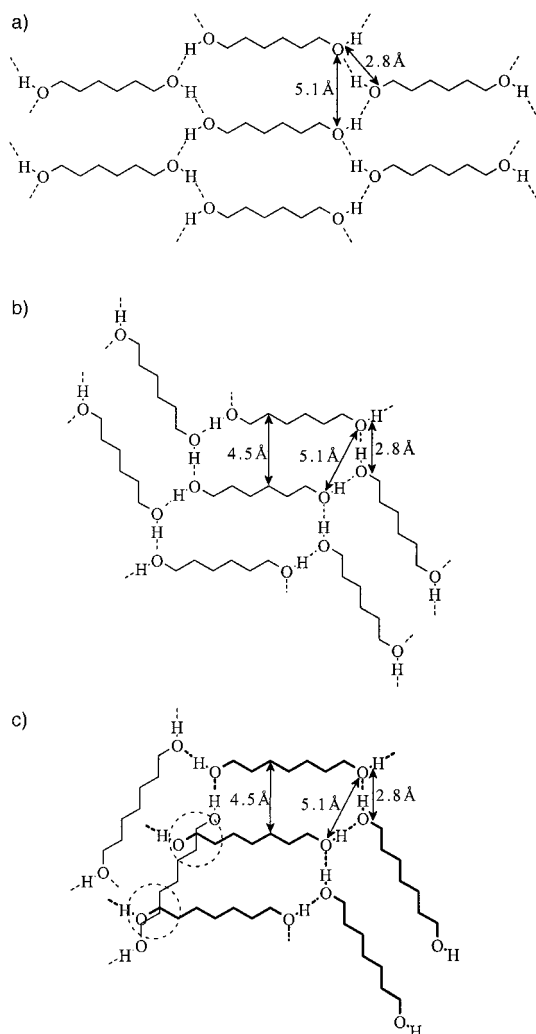


Figure 3. a) Hypothetical layer structure sustained by  $\text{O}-\text{H}\cdots\text{O}$  hydrogen-bonded chains in diols (shown here for an even diol). b) Offset of even diol molecules within a column driven by the intergrooving pattern of hydrophobic interactions. The magnitude of the offset (2.4 Å) is the same as the distance between alternate  $\text{CH}_2$  groups. c) Geometrical hindrance of molecular offset in odd diols (conflicting areas are highlighted in dashed circles). The  $\text{O}-\text{H}\cdots\text{O}$  chains can only be formed at one of the ends.

(Figures 3 b and 4). The molecules are offset along their length such that the  $\alpha\text{-CH}_2$  groups fit into the penultimate grooves, and adjacent columns are inclined to preserve the  $\text{O}-\text{H}\cdots\text{O}$  chains. The offset also allows the  $\beta\text{-CH}_2$  groups to fit into the supramolecular grooves formed by  $\text{CH}_2-\text{O}-\text{H}\cdots\text{O}$  (Figure 4), leading to a dense packing with hydrocarbon chains separated by 4.5 Å (c.f. 4.7 Å in *n*-alkanes).

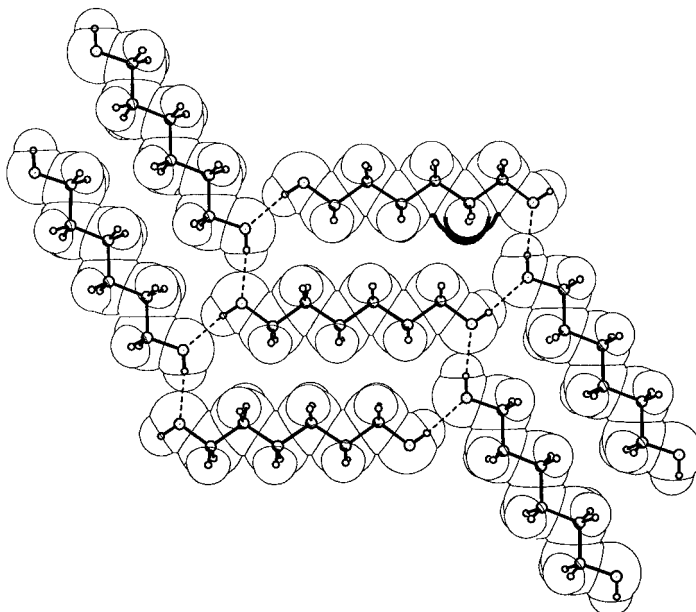


Figure 4. Layer structure in even diols illustrated with the structure of 1,6-hexanediol. Notice the offset of molecules within the columns and the fit of  $\beta\text{-CH}_2$  groups into the supramolecular grooves formed by  $\text{CH}_2-\text{O}-\text{H}\cdots\text{O}$  (marked with thick lines).

However, a similar offset packing is not possible in odd diols. Whereas the all-*trans* conformation in even diols leads to an antiparallel projection of the two  $\text{C}-\text{O}$  groups, in odd diols it projects the two  $\text{C}-\text{O}$  groups in the same direction, thus precluding the formation of  $\text{O}-\text{H}\cdots\text{O}$  chains at opposite ends of the molecule (Figure 3 c). In fact, in the odd diols one of the  $\text{C}-\text{O}$  groups adopts a *gauche* conformation, leading to a three-dimensional network (Figure 5)<sup>[12]</sup> in which the packing of the hydrophobic moiety is not as effective as in the even diols. The odd diols are thus less densely packed than the even ones.<sup>[13]</sup>

Like the OH groups, the  $\text{NH}_2$  groups also act as hydrogen-bond donors and acceptors simultaneously, and extend to a chain pattern in the diamine structures.<sup>[10]</sup> The layer structure in even diamines is similar to that in even diols (Figure 6), but the  $\text{N}\cdots\text{N}$  separation (3.2 Å) is generally longer than the  $\text{O}\cdots\text{O}$  separation (2.8 Å). Thus, adjacent molecules are now spaced at 5.2 Å, a distance at which the hydrophobic packing pattern of the even diols or *n*-alkanes would leave much empty space. The hydrocarbon chain therefore swivels with respect to the fulcrum of the hydrogen-bonded chain (around the main molecular axis by 45°) to fill the gaps (compare Figures 4 and 6).

As described for odd diols, odd diamines cannot adopt the offset packing. Nevertheless, unlike odd diols, odd diamines

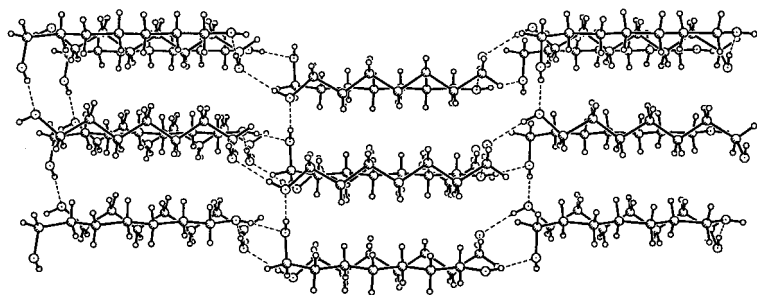


Figure 5. Crystal structure of 1,7-heptanediol illustrating the three-dimensional networking of O–H...O hydrogen bonds in odd diols. Notice that one of the C–O groups adopts a *gauche* conformation.

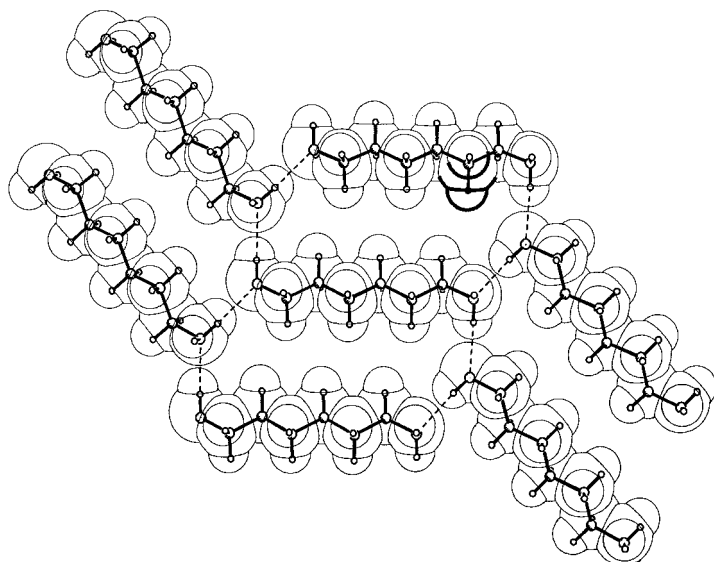


Figure 6. Layer structure in even diamines illustrated with the structure of 1,6-hexanediamine. Notice the offset of molecules within the columns and the fit of  $\beta$ -CH<sub>2</sub> groups into the supramolecular grooves formed by CH<sub>2</sub>–N–H...N (marked with thick lines). Attention is also called to the swiveling of molecules with respect to the layer plane (compare with Figure 4).

form a layer structure with N–H...N chains, but without the offset of the molecules within a column (Figure 7). This layer is analogous to the hypothetical layer depicted in Figure 3a. Adjacent molecules within a column are now separated by 5.7 Å. Even after the swiveling of the hydrocarbon chain, the

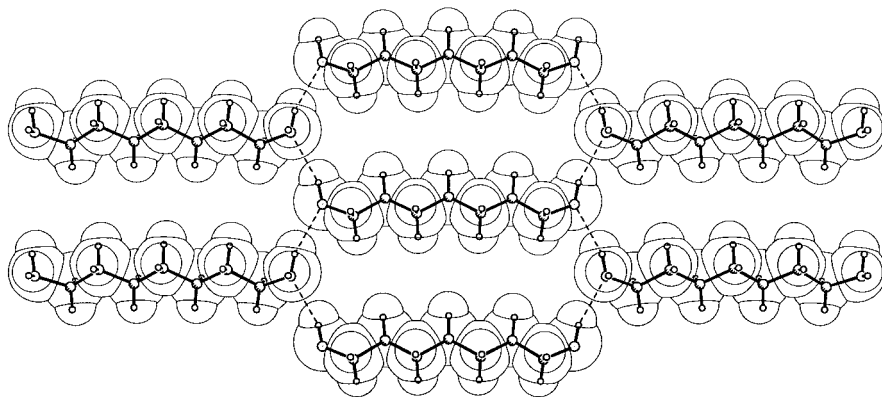


Figure 7. Layer structure in odd diamines illustrated with the structure of 1,7-heptanediamine. Notice the similarity to Figure 3a and the absence of the offset as well as the swiveling of molecules with respect to the layer plane (compare with Figure 6).

odd diamines are less densely packed than the even ones.<sup>[13]</sup> We note that the interlayer packing in even and odd diamines is similar, with the second NH group forming a longer N–H...N hydrogen bond between the layers.

Lattice energy calculations have been made for all the structures reported here.<sup>[14]</sup> The contributions from hydrogen-bond and van der Waals interactions are recorded in Table 1. While hydrogen bond energies are similar within each series, the van der Waals energies are greater for even members and show an alternation similar to that of the melting points in both series. It is therefore the difference in hydrophobic packing that causes the alternation of melting points.

The packing patterns in 1,2-ethanediol, 1,3-propanediol, and 1,2-ethanediamine are different from those described here because in these lower members the hydrogen bonds overrule the hydrophobic interactions.

The analysis of the crystal structures of diols and diamines has revealed the interplay between two important intermolecular interactions that are possible in these amphiphilic compounds, namely, hydrogen bonding and hydrophobic interactions. While hydrogen bonding and hydrophobic interactions operate in consonance in even members, and therefore culminate in dense packing, they run into geometrical conflicts in odd members, leading to looser packing. Accordingly, the odd members of the diol and diamine series have relatively lower densities and melting points than the even members.<sup>[15, 16]</sup>

Received: August 30, 1999 [Z13939]

- [1] G. A. Jeffrey, W. Saenger, *Hydrogen Bonding in Biological Structures*, Springer, Berlin, **1991**.
- [2] a) T. E. Creighton, *Proteins: Structures and Molecular Principles*, Freeman, New York, **1987**; b) A. M. Davis, S. J. Teague, *Angew. Chem.* **1999**, *111*, 778; *Angew. Chem. Int. Ed.* **1999**, *38*, 736; c) C. Tanford, *The Hydrophobic Effect: Formation of Micelles and Biological Membranes*, Wiley, New York, **1973**; d) A. Ullman, *Chem. Rev.* **1996**, *96*, 1533; e) R. S. Clegg, J. E. Hutchison, *J. Am. Chem. Soc.* **1999**, *121*, 5319; f) J.-M. Lehn, *Supramolecular Chemistry: Concepts and Perspectives*, VCH, Weinheim, **1995**; g) J. Wang, F. Leveiller, D. Jacquemain, K. Kjaer, J. Als-Nielsen, M. Lahav, L. Leiserowitz, *J. Am. Chem. Soc.* **1994**, *116*, 1192; h) Y. Xia, G. M. Whitesides, *Angew. Chem.* **1998**, *110*, 568; *Angew. Chem. Int. Ed.* **1998**, *37*, 550.
- [3] G. R. Desiraju, *Angew. Chem.* **1995**, *107*, 2541; *Angew. Chem. Int. Ed. Engl.* **1995**, *34*, 2311.
- [4] A. I. Kitaigorodskii, *Molecular Crystals and Molecules*, Academic Press, New York, **1973**.
- [5] F. L. Breusch, *Fortschr. Chem. Forsch.* **1969**, *12*, 119.
- [6] R. Boese, H. C. Weiss, D. Bläser, *Angew. Chem.* **1999**, *111*, 1042; *Angew. Chem. Int. Ed.* **1999**, *38*, 988.
- [7] a) R. Boese, M. Nussbaumer in *Organic Crystal Chemistry*, Vol. 7 (Eds.: D. W. Jones, A. Katrusiak), Oxford University Press, Oxford, **1994**, pp. 20–37; b) V. R. Thalladi,

- H. C. Weiss, D. Bläser, R. Boese, A. Nangia, G. R. Desiraju, *J. Am. Chem. Soc.* **1998**, *120*, 8702; c) For further details, see: <http://www.ohcd-system.com>.
- [8] Crystal structure analyses: The data were collected at 130 K either on a Nicolet R3 or on a SMART diffractometer using MoK $\alpha$  radiation. The data were corrected for cylindrical shape for crystals grown in situ. Structure solution by direct methods and refinements on F<sup>2</sup> with SHEXLTL-Plus (Version 5.03). All non-hydrogen atoms were refined anisotropically. The positions of the hydrogen atoms were taken from a difference Fourier map and refined isotropically without constraints. a) 1,3-Propanediol: space group  $P2_1/n$ ,  $2\theta_{\max} = 60^\circ$ , reflections measured: 1255, independent: 1200, observed ( $I > 2\sigma_I$ ): 951, 78 parameters,  $R1 = 0.046$ ,  $wR2 = 0.153$ , residual electron density  $+0.39/-0.20$  e Å<sup>-3</sup> (CCDC-132862); b) 1,4-butanediol: space group  $P2_1/n$ ,  $2\theta_{\max} = 55^\circ$ , reflections measured: 2432, independent: 1134, observed ( $I > 2\sigma_I$ ): 964, 95 parameters,  $R1 = 0.063$ ,  $wR2 = 0.164$ , residual electron density  $+0.45/-0.51$  e Å<sup>-3</sup> (CCDC-132863); c) 1,5-pentanediol: space group  $P2_12_12_1$ ,  $2\theta_{\max} = 60^\circ$ , reflections measured: 3628, independent: 1774, observed ( $I > 2\sigma_I$ ): 1632, 112 parameters,  $R1 = 0.031$ ,  $wR2 = 0.084$ , residual electron density  $+0.26/-0.17$  e Å<sup>-3</sup> (CCDC-132864); d) 1,6-hexanediol: space group  $P2_1/n$ ,  $2\theta_{\max} = 60^\circ$ , reflections measured: 1455, independent: 1206, observed ( $I > 2\sigma_I$ ): 911, 129 parameters,  $R1 = 0.045$ ,  $wR2 = 0.134$ , residual electron density  $+0.26/-0.22$  e Å<sup>-3</sup> (CCDC-132865); e) 1,7-heptanediol: space group  $P2_12_12_1$ ,  $2\theta_{\max} = 60^\circ$ , reflections measured: 1908, independent: 1883, observed ( $I > 2\sigma_I$ ): 1313, 144 parameters,  $R1 = 0.058$ ,  $wR2 = 0.151$ , residual electron density  $+0.24/-0.28$  e Å<sup>-3</sup> (CCDC-132866); f) 1,8-octanediol: space group  $P2_1/n$ ,  $2\theta_{\max} = 60^\circ$ , reflections measured: 3510, independent: 1248, observed ( $I > 2\sigma_I$ ): 1084, 82 parameters,  $R1 = 0.036$ ,  $wR2 = 0.097$ , residual electron density  $+0.33/-0.22$  e Å<sup>-3</sup> (CCDC-132867); g) 1,9-nonanediol: space group  $P2_12_12_1$ ,  $2\theta_{\max} = 60^\circ$ , reflections measured: 3544, independent: 2603, observed ( $I > 2\sigma_I$ ): 1357, 180 parameters,  $R1 = 0.072$ ,  $wR2 = 0.158$ , residual electron density  $+0.47/-0.22$  e Å<sup>-3</sup> (CCDC-132868); h) 1,2-ethanediol: space group  $P2_1/c$ ,  $2\theta_{\max} = 60^\circ$ , reflections measured: 1614, independent: 520, observed ( $I > 2\sigma_I$ ): 477, 35 parameters,  $R1 = 0.065$ ,  $wR2 = 0.166$ , residual electron density  $+0.78/-0.45$  e Å<sup>-3</sup> (CCDC-132869); i) 1,3-propanediol: space group  $Cmc2_1$ ,  $2\theta_{\max} = 60^\circ$ , reflections measured: 1504, independent: 502, observed ( $I > 2\sigma_I$ ): 477, 47 parameters,  $R1 = 0.032$ ,  $wR2 = 0.082$ , residual electron density  $+0.19/-0.28$  e Å<sup>-3</sup> (CCDC-132870); j) 1,4-butanediol: space group  $Pbca$ ,  $2\theta_{\max} = 60^\circ$ , reflections measured: 3172, independent: 794, observed ( $I > 2\sigma_I$ ): 745, 52 parameters,  $R1 = 0.042$ ,  $wR2 = 0.120$ , residual electron density  $+0.23/-0.26$  e Å<sup>-3</sup> (CCDC-132871); k) 1,5-pentanediol: space group  $Cmc2_1$ ,  $2\theta_{\max} = 60^\circ$ , reflections measured: 3600, independent: 972, observed ( $I > 2\sigma_I$ ): 892, 64 parameters,  $R1 = 0.039$ ,  $wR2 = 0.104$ , residual electron density  $+0.24/-0.24$  e Å<sup>-3</sup> (CCDC-132872); l) 1,6-hexanediol: space group  $Pbca$ ,  $2\theta_{\max} = 60^\circ$ , reflections measured: 1249, independent: 1069, observed ( $I > 2\sigma_I$ ): 899, 69 parameters,  $R1 = 0.061$ ,  $wR2 = 0.177$ , residual electron density  $+0.55/-0.31$  e Å<sup>-3</sup> (CCDC-132873); m) 1,7-heptanediol: space group  $Cmc2_1$ ,  $2\theta_{\max} = 60^\circ$ , reflections measured: 3114, independent: 1159, observed ( $I > 2\sigma_I$ ): 1067, 81 parameters,  $R1 = 0.032$ ,  $wR2 = 0.095$ , residual electron density  $+0.36/-0.17$  e Å<sup>-3</sup> (CCDC-132874); n) 1,8-octanediol: space group  $Pbca$ ,  $2\theta_{\max} = 45^\circ$ , reflections measured: 1098, independent: 593, observed ( $I > 2\sigma_I$ ): 449, 86 parameters,  $R1 = 0.031$ ,  $wR2 = 0.084$ , residual electron density  $+0.08/-0.14$  e Å<sup>-3</sup> (CCDC-132875). Crystallographic data (excluding structure factors) for the structures reported in this paper have been deposited with the Cambridge Crystallographic Data Centre as supplementary publication nos. CCDC-132862 to CCDC-132874. Copies of the data can be obtained free of charge on application to CCDC, 12 Union Road, Cambridge CB2 1EZ, UK (fax: (+44) 1223-336-033; e-mail: deposit@ccdc.cam.ac.uk).
- [9] The crystal structures of some of the compounds studied here have been reported. The analyses were carried out at different temperatures and sometimes to lower accuracies: a) 1,2-ethanediol at 130 K: R. Boese, H. C. Weiss, *Acta Crystallogr. Sect. C* **1998**, *54*, 24; b) 1,6-hexanediol at 300 K: M. Lindgren, T. Gustafsson, J. Westerling, A. Lund, *Chem. Phys.* **1986**, *106*, 441; c) 1,9-nonanediol and 1,10-decanediol at 100 K: ref. [2g]; d) 1,2-ethanediol at 210 K: S. Jamet-Delcroix, *Acta Crystallogr. Sect. B* **1973**, *29*, 977; e) 1,6-hexanediol at 300 K: W. P. Binnie, J. M. Robertson, *Acta Crystallogr.* **1950**, *3*, 424; f) 1,7-heptanediol at 210 K: R. Gotthardt, J. H. Fuhrhop, J. Buschmann, P. Luger, *Acta Crystallogr. Sect. C* **1997**, *53*, 1715.
- [10] C. P. Brock, L. L. Duncan, *Chem. Mater.* **1994**, *6*, 1307.
- [11] V. R. Thalladi, H.-C. Weiss, R. Boese, A. Nangia, G. R. Desiraju, *Acta Crystallogr. Sect. B* **1999**, *55*, 1005, and references therein.
- [12] The geometries of the O–H...O bonds are similar at the two ends of the molecules, which also holds for C4 and C6-diols where  $Z' = 1$ .
- [13] This is further corroborated by the fact that the calculated packing fractions for even diols and even diamines are systematically higher than those for the corresponding odd members (Table 1) and exhibit an alternating trend similar to that of the melting points and densities.
- [14] We have used the Dreiding-II force field built-in the crystal packer module of the Cerius<sup>2</sup> program. All calculations were performed as the snapshots of crystal structures. The overall result is the same even after the crystal structures were minimized.
- [15] One of the C–O groups adopts a strained *gauche* conformation in odd diols in the solid state, which also contributes to the lowering of the melting points of odd diols.
- [16] Increased hydrophobicity does not alter the structural patterns in diols. Higher analogues of even and odd diols (a) 1,11-undecanediol: N. Nakamura, S. Setodoi, T. Ikeya, *Acta Crystallogr. Sect. C* **1999**, *55*, 789; b) 1,12-dodecanediol: N. Nakamura, S. Setodoi, *Acta Crystallogr. Sect. C* **1997**, *53*, 1883; c) 1,13-tridecanediol: N. Nakamura, Y. Tanihara, T. Takayama, *Acta Crystallogr. Sect. C* **1997**, *53*, 253; d) 1,16-hexadecanediol: N. Nakamura, T. Yamamoto, *Acta Crystallogr. Sect. C* **1994**, *50*, 946) adopt structures isomorphous to their lower analogues.

## Bridged Cyclic Oligoribonucleotides as Model Compounds for Codon–Anticodon Pairing\*\*

Ronald Micura,\* Werner Pils, and Karl Grubmayr

Dedicated to Professor Albert Eschenmoser  
on the occasion of his 75th birthday

The base sequences of genes are translated with complementary mRNA and the assistance of tRNAs into protein sequences. This process takes place at the ribosome.<sup>[1]</sup> Thereby, the formation of specific Watson–Crick base pairs between codon (mRNA) and anticodon (tRNA) is crucial. The structure of the corresponding pairing complex is similar to a double helical A-form RNA.<sup>[2,3]</sup> Although in general,

[\*] Dr. R. Micura,<sup>[+]</sup> Dipl.-Ing. W. Pils, a. Univ.-Prof. Dr. K. Grubmayr  
Institut für Chemie  
Johannes Kepler Universität Linz  
Altenbergerstrasse 69, 4040 Linz (Austria)  
Fax: (+43) 732-2468-747  
E-mail: micura@gmx.net

[+] Alternative address:  
Laboratorium für Organische Chemie der Eidgenössischen Technischen Hochschule  
Universitätstrasse 16, 8092 Zürich (Switzerland)  
Fax: (+41) 1-632-1043

[\*\*] R.M. acknowledges the Austrian Academy of Science for an APART fellowship (Austrian Programme for Advanced Research and Technology). This work was supported by the Austrian Science Fund, Vienna (P13216-CHE). R.M. is obliged to Prof. Eschenmoser (Zürich) and Prof. Falk (Linz) for generous hospitality in their laboratories. We thank Dr. Krishnamurthy (Scripps Institute, La Jolla, California) for mass analyses and Dr. Weiss (Xeragon AG, Zürich) for 2'-O-TOM-phosphoramidites of standard bases.